Multilevel 2D-3D Intensity-Based Image Registration

Annkristin Lange$^{(\boxtimes)}$ and Stefan Heldmann

Fraunhofer MEVIS, Lübeck, Germany
`annkristin.lange@mevis.fraunhofer.de`

Abstract. 2D-3D image registration is an important task for computer-aided minimally invasive vascular therapies. A crucial component for practical image registration is the use of multilevel strategies to avoid local optima and to speed-up runtime. However, due to the different dimensionalities of the 2D fixed and 3D moving image, the setup of multilevel strategies is not straightforward.

In this work, we propose an intensity-driven 2D-3D multiresolution registration approach using the normalized gradient fields (NGF) distance measure. We discuss and empirically analyze the impact on the choice of 2D and 3D image resolutions. Furthermore, we show that our approach produces results that are comparable or superior to other state-of-the-art methods.

Keywords: 2D-3D registration · Multilevel · Multiresolution · Normalized gradient fields · Vascular images

1 Introduction

Minimally invasive endovascular therapies are nowadays part of standard routine for many diseases of the vascular system. Before an intervention usually a planning CT with contrast agent is done. The navigation of the catheter through the vascular system during the intervention can be quite challenging, even if fluoroscopy images are obtained. Registration of 2D projection images to a 3D planning CT image provides more information and allows to reduce intervention time, radiation exposure and amount of contrast agent [1].

A nice overview about the topic of 2D-3D registration and classification of the different strategies developed over the years can be found in [6]. The strategies can roughly be divided into feature- and intensity-based methods. Intensity-based approaches rely on synthetic projections from the 3D planning volume that mimic the real projection process, so-called digitally reconstructed radiographs (DRRs). The registration is then based on the comparison between the DRRs and the measured projections. In contrast, feature-based methods attempt to align features computed from, e.g. gradients [7,8], surface/contour points [12] or directly from the images.

An important component for any practical image registration scheme is the use of multilevel strategies to avoid local optima and speed-up the registration [5]. The general idea behind multilevel strategies is, that coarser resolution mainly carry global image information and features, and local details gradually become present with finer resolutions, i.e. more details are added. On that account, registration is performed level-wise from coarse-to-fine and solutions from one level are used as initial guess for finding the solution at the next finer level.

However, in 2D-3D registration the application of multilevel strategies is not as straightforward as for the registration of images with same dimensionality. Here we compare given 2D projection images with DRRs created from 3D volume data. Clearly, coarsening and projecting do not commute, i.e. creating a coarse resolution 2D image from a given 2D projection image, e.g., by downsampling, is different from projecting a 3D coarse resolution image.

Nevertheless multilevel strategies are successfully employed in many 2D-3D registration methods (see [6] for a list of publications). To best of our knowledge, no work has been done on the relation of the resolutions between 2D images and 3D volumes. In [3] few experiments regarding the choice of resolutions are performed and [9] presents a general discussion motivating the use of multilevel strategies in 2D-3D registration. However, the relationship between the resolutions of the volumes and projections is not discussed.

In this work we present a multilevel 2D-3D registration with the so-called normalized gradient field distance measure (NGF) [2]. The focus of the paper is on the relation and the choice of resolutions for 2D and 3D image data.

2   Methods

In the following we describe our multilevel 2D-3D registration method. We start with the description of computing 2D projection images in Sect. 2.1. Subsequent we present our intensity-based 2D-3D image registration with the NGF distance measure in Sect. 2.2 and finally, we discuss our multilevel strategy in Sect. 2.3.

2.1   Digitally Reconstructed Radiographs (DRRs)

We consider X-ray imaging as the process of measuring the attenuation of radiation, that is emitted from a radiation point source located at position q with the initial energy I_0. Mathematically, this can be modeled by a projection operator $\mathcal{P}$ that maps a 3D attenuation map $\mu : \mathbb{R}^3 \to \mathbb{R}$ to a 2D image. Therefore, let $x \in \mathbb{R}^2$ be a location in the 2D projection image and let $d(x) \in \mathbb{R}^3$ be the location of the corresponding detector element in 3D-space. Then the projection is given by

$$\mathcal{P}[\mu](x) := I_0 \exp\left(-\int_{L(q,d(x))} \mu \, ds\right) \tag{1}$$

where $L(q, d(x)) := \{q + t(d(x) - q) \mid t \in [0,1]\}$ is the line from the radiation source q to the detector element $d(x)$. Theoretically, there exists an affine relationship between the attenuation map μ and the CT image, so we can estimate

μ from the CT intensity values. Furthermore, to accelerate the computationally expensive calculation of these synthetic projections, the so-called digitally reconstructed radiographs (DRR), we have implemented a GPU version.

2.2   Intensity-Based 2D-3D Image Registration

A common approach is to model d-dimensional images as intensity mappings, i.e. an image $I : \mathbb{R}^d \to \mathbb{R}$ that maps a position $x \in \mathbb{R}^d$ to an intensity $I(x)$. Image registration can then be described as the process of finding a plausible spatial transformation y such that the transformation applied to a given template image $T(y)$ is similar to a given reference image R, i.e. $T(y(x)) \approx R(x)$. To describe the similarity between the images, a suitable cost-function the so-called distance measure $\mathcal{D}$ is used. Then, the registration problem can be defined as a minimization problem $\mathcal{D}(R, T(y)) = \min$.

Unlike classical image registration, where reference and template image have same dimensionality, in 2D-3D registration the reference image $R : \mathbb{R}^2 \to \mathbb{R}$ is a 2D measured projection image while the template image $T : \mathbb{R}^3 \to \mathbb{R}$ still is a 3D image. Accordingly, the desired transformation is also a 3D mapping $y : \mathbb{R}^3 \to \mathbb{R}^3$. The similarity is then measured between the 2D reference image and a 2D DRR $\mathcal{P}[T(y)]$ of the deformed 3D template image $T(y) := T \circ y$ and the minimization problem for image registration becomes $\mathcal{D}(R, \mathcal{P}[T(y)]) = \min$. In this work we used the normalized gradient field (NGF) distance measure [2,10]. For two 2D images $R, \widetilde{T} : \mathbb{R}^2 \to \mathbb{R}$, it is given by

$$\text{NGF}(R, \widetilde{T}) = \int_\Omega 1 - \left(\frac{\langle \nabla R(x), \nabla \widetilde{T}(x) \rangle_{\varepsilon_R \varepsilon_T}}{\|\nabla R(x)\|_{\varepsilon_R} \|\nabla \widetilde{T}(x)\|_{\varepsilon_T}} \right)^2 dx \qquad (2)$$

with $\langle x, y \rangle_\varepsilon := x^\top y + \varepsilon$, $\|x\|_\varepsilon = \sqrt{\langle x, x \rangle_{\varepsilon^2}}$, domain $\Omega \subset \mathbb{R}^2$, that models the 2D field-of-view of the detector and so-called edge parameters $\varepsilon_R, \varepsilon_T > 0$.

In order to find plausible deformations, the search space of admissible transformations can be restricted. Here, we only allow for translations and rotations, i.e. rigid transformations $y(x) = Qx + b$ with 3-by-3 rotation matrix $Q \in SO(3)$ and translation vector $b \in \mathbb{R}^3$. As the rotation matrix can be parameterized by three rotation angles, we obtain a six-parameter deformation model $y \equiv y_\theta$ with the parameters $\theta \in \mathbb{R}^6$. Summarizing, our intensity-based rigid 2D-3D registration approach is

$$\min_{\theta \in \mathbb{R}^6} \text{NGF}\left(R, \mathcal{P}[T(y_\theta)]\right) \qquad (3)$$

To solve the optimization problem numerically, a Gauss-Newton optimization scheme with backtracking Armijo linesearch and analytically computed gradients is used. In the DRR computation a radial sampling with uniform step length is used.

2.3   Multilevel Strategy

The idea of any multilevel strategy is to represent a given problem on coarse resolutions with less detail, which allows for efficient solving and, above all,

adds to finding solutions close to a global optimum of the original problem. Starting from a coarsest level, a solution for the coarse problem is computed and subsequently prolongated to the next finer level, where it serves as an initial guess for the optimization. The process is then continued until the finest level is reached.

The common approach in intensity-based image registration to represent the problem at coarse resolutions is to create low resolution versions of the given input image data, e.g. by downsampling or averaging pixels. We also follow this approach here. To this end, let R be the given 2D image, I_ℓ^{2D} be an operator that maps a 2D image to the resolution at ℓ-th level and let $R_\ell := I_\ell^{2D}[R]$. In the same way let T be the given 3D volume and $T_\ell := I_\ell^{3D}[T]$ with an operator I_ℓ^{3D} which maps a 3D image to a 3D image with the resolution for the ℓ layer. Now, we have two generic options to setup the registration problem at the ℓ-th level. First, we could search for a transformation y such that $\mathrm{NGF}(R_\ell, I_\ell^{2D}[\mathcal{P}[T(y)]]) = \min$. Another option is to look for minimizers of $\mathrm{NGF}(R_\ell, \mathcal{P}[T_\ell(y)])$. Clearly, projection and coarsening do not commute in general, i.e. $I_\ell^{2D}[\mathcal{P}[T]] \neq \mathcal{P}[I_\ell^{3D}[T]] = \mathcal{P}[T_\ell(y)]$ and we cannot expect that solutions for both problems coincide. Although the first approach seems more natural from a conceptual point of view, it is computationally demanding as it requires the computation of high quality projections at the original (finest) image resolution regardless of the resolution of the problem. Furthermore, we need to incorporate the projection operator I_ℓ^{2D} into our numerics, e.g., for computing derivatives. For this reason, we stick to the second approach.
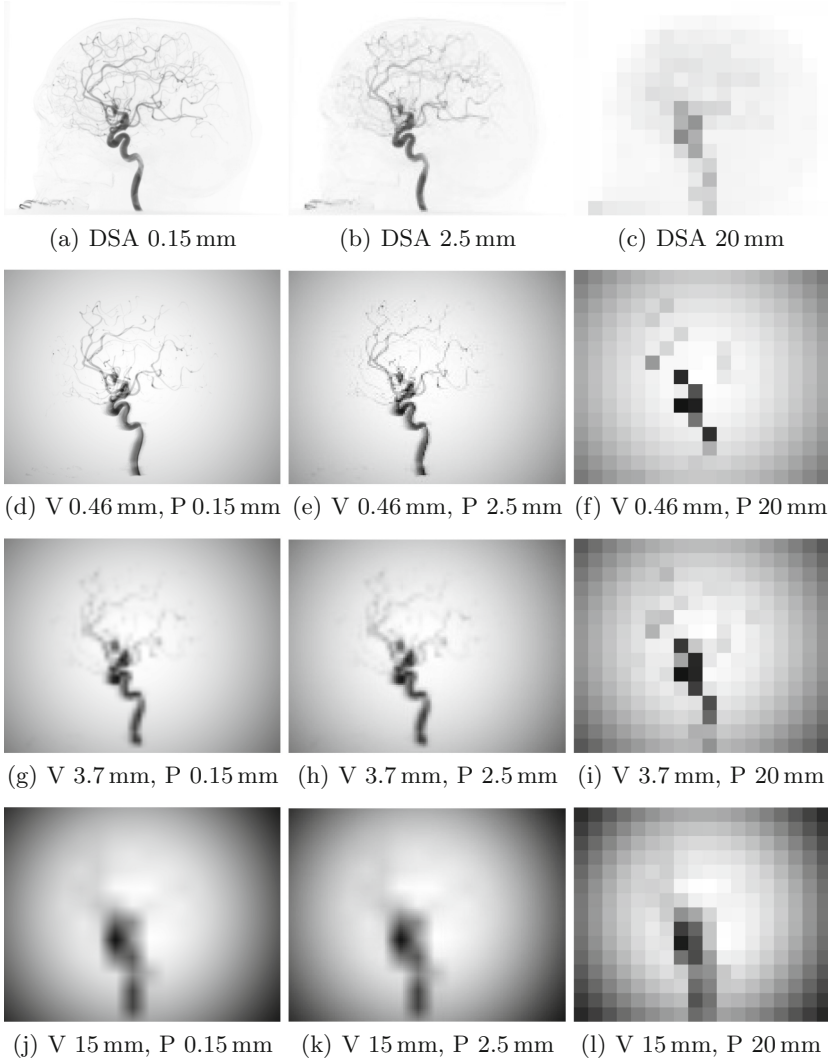
Accordingly, we create image pyramids for the given input images by averaging neighboring pixels and voxels, respectively, so that the resolutions double from a coarse to the next finer level. Then, starting at coarsest level, we compute solutions to (2.3) using the data of the current level and the solution from the previous level as an initial guess. Our overall scheme can be summarized as follows:

1. Create R_ℓ, T_ℓ for $\ell = 1, \ldots, L$ from coarsest ($\ell = 1$) to finest ($\ell = L$) level
2. Choose initial guess y_0 for coarsest level
3. `for` level $\ell = 1, .., L$ `do`

   Use $y_{\ell-1}$ as initial guess for finding y_ℓ such that

$$\mathrm{NGF}\left(R_\ell, \mathcal{P}[T_\ell(y_\ell)]\right) \overset{!}{=} \min$$

   `end`

An important point with substantial impact on registration results, is the choice and alignment of the resolutions of 2D image and 3D projection data. The issue is illustrated in Fig. 1 showing 2D-DSA reference images R_ℓ and DRRs, i.e. projected 3D volumes $\mathcal{P}[T_\ell]$, for different resolutions. There is no obvious answer to the question what combination of resolutions to pick for optimal registration results. Besides evaluating and comparing our method with others, we focus on the analysis of this question with our experiments presented in the next section.

(a) DSA 0.15 mm   (b) DSA 2.5 mm   (c) DSA 20 mm

(d) V 0.46 mm, P 0.15 mm (e) V 0.46 mm, P 2.5 mm (f) V 0.46 mm, P 20 mm

(g) V 3.7 mm, P 0.15 mm (h) V 3.7 mm, P 2.5 mm (i) V 3.7 mm, P 20 mm

(j) V 15 mm, P 0.15 mm   (k) V 15 mm, P 2.5 mm   (l) V 15 mm, P 20 mm

Fig. 1. Calculated DRRs from lateral view with different resolutions of the volume (changing from fine to coarse from top to bottom) and the projections (changing from fine to coarse from left to right). The 2D-DSAs with the same projection resolutions are given for comparison.

3   Experiments and Evaluation

In the following we will experimentally analyze how image resolutions for our 2D-3D multilevel registration can be selected and related. We will also investigate the choice of the finest resolution. Furthermore, we will compare our proposed 2D-3D multilevel registration method using the NGF distance measure with various state-of-the-art methods.

3.1   Clinical Database

Our evaluation is based on the public available clinical data presented in [7]. The data consists of images from 10 patients with cerebral vascular diseases such as aneurysms. Each data set contains a 3D digitally subtracted rotational angiogram (3D-DSA) volume, 2D digitally subtracted angiograms (2D-DSA) from lateral (LAT) and anterior-posterior (AP) views and a rigid gold standard transformation for the 3D volume. The gold standard transformations were derived from fiducial markers and have predicted mean target registration errors (mTRE) ranging from 0.033 to 0.056 mm [7]. In addition, landmarks and initial transformations are provided for comparative evaluation. The original image size of the 3D-DSA is $512 \times 512 \times 391$ voxel with an isotropic resolution of 0.4646 mm. The image size for the 2D-DSA ranges from 1920 to 2480 pixel with an isotropic resolution of 0.154 mm.

3.2   Evaluation Parameters

Error measures based on landmarks are often used to determine the quality of a registration. Two measures commonly used in 2D-3D registration are the mean Target Registration Error (mTRE) and the mean Re-Projection Distance (mRPD) [4]. Given N landmarks $x_1, ..., x_N \in \mathbb{R}^3$, the mTRE between transformation y_{reg} and gold standard y_{gold} is given by

$$\text{mTRE} = \frac{1}{N} \sum_{i=1}^{N} \|y_{\text{reg}}(x_i) - y_{\text{gold}}(x_i)\|. \tag{4}$$

The mRPD measures the distance of the ray passing through source q and transformed landmark to gold standard. It is defined as

$$\text{mRPD} = \frac{1}{N} \sum_{i=1}^{N} \min_{z \in L(q, y_{\text{reg}}(x_i))} \|z - y_{\text{gold}}(x_i)\| \tag{5}$$

where $L(q, y_{\text{reg}}(x_i))$ is the line passing through the source q and the registered landmark $y_{\text{reg}}(x_i)$.

3.3   Experiments

For almost all experiments we used the set of 400 initial displacements that was specified for each dataset. The mTRE of the displacements ranges from 0 mm to 20 mm, so that each interval of 1 mm contains 20 displacements. The displacements were generated by randomly translating about $(-20 \text{ mm}, 20 \text{ mm})$ and rotating around $(-10°, 10°)$ all three axes. Similar to [7] the validation criteria are the percentage of successful registration (SR), the mean and standard deviation of all successful registrations and the capture range (CR). A registration is viewed as successful, if the mTRE is less then 2 mm, which is approximately the radius of the larger cerebral vessels. The capture range is defined as the first interval in which less than 95% of the registrations are successful.

Registration with Original Resolution. Initially, we started our analysis with an experiment in which we perturbed a given gold standard transformation with a shift of 5 mm each along the in-plane axes x and y, resulting in an mTRE before registration of 7.1 mm. For this and the following experiments results were best, if on the coarsest level the resolution of the volume was around 15 mm. Using coarser levels did not achieve improvements, whereas using less levels led to a smaller capture range. The registration was then done for different combinations of finest resolutions. The number of levels depend on that choice as the coarser resolutions are computed from there. If, for example, a fine resolution of 0.93 mm for the volume and 0.31 mm for the projection is selected, the registration is performed on five levels, starting with the coarsest volume resolution of 15 mm and projection resolution of 5 mm (i.e. along the diagonal in Fig. 2(a): (5, 15), (2.5, 7.5), (1.2, 3.7), (0.62, 1.86), (0.31, 0.93)).

Our results show, that we obtain best results when the resolution of the projection is similar or slightly coarser than the resolution of the volume, see Fig. 2(a). It is noticeable that the registration with finest available but also quite different resolutions of 2D projection and 3D volume basically fails. In a next step we reviewed the result based on the set of given initial displacements (cf. Table 1). When using the original resolution of 2D-DSA and 3D-DSA as finest level, the results are not convincing, especially the capture range of only 3 mm is small. Much better results are obtained when not the finest resolution of the projection but the second or even third finest was used. In this case the capture

mTRE		Volume					
	Res (mm)	0.46	0.93	1.86	3.7	7.5	15
	0.15	44.6	138.2	418.4	515.9	985.0	450.0
	0.31	2.7	45.4	137.7	421.3	469.0	430.9
	0.62	1.2	2.7	44.4	138.1	403.9	339.8
	1.2	1.1	1.1	2.8	47.5	157.8	250.6
Projection	2.5	1.6	1.3	1.0	6.3	72.5	102.8
	5	7.1	2.1	1.5	2.7	24.6	54.4
	10	12.4	11.7	7.7	3.5	12.1	41.3
	20	15.8	11.8	12.7	21.1	17.1	36.7

(a) Original resolution

mTRE		Volume					
	Res (mm)	0.46	0.93	1.86	3.7	7.5	15
	0.46	1.1	5.9	74.3	230.3	862411.3	463.9
	0.93	1.1	1.0	6.6	81.1	231.1	277.2
	1.86	1.3	1.3	0.9	11.7	100.2	152.5
Projection	3.7	3.5	1.9	1.4	2.6	27.1	98.5
	7.5	9.4	7.2	4.1	3.0	9.4	47.7
	15	12.1	12.9	14.1	21.6	12.3	16.3

(b) Resampled projections

Fig. 2. mTRE (in mm) values for a registration of a 2D-DSA to a 3D-DSA averaged over all 10 datasets with an initial translation along the in-plane axes $(x, y) = (5\,\text{mm}, 5\,\text{mm})$ with different resolutions of the projection and the volume.

range is 12 and 16 mm, respectively and the success rate is around 96% instead of 68% with no loss of accuracy. The mTRE is in all three cases around 1.1 mm and the mRPD is 0.17 mm.

Summarizing, the results of this experiment led to the assumption that the best registration results are achieved when the resolution of the projection and the volume are comparable, as it is more or less the case for the second and third finest resolution of the projection compared to the finest resolution of the volume.

Table 1. Results for the registration of a 3D-DSA to a 2D-DSA from LAT view averaged over all 10 datasets for different finest resolutions of the 2D-DSA.

Resolution finest level		SR (%)	mTRE (mm)	mRPD (mm)	CR (mm)	Time (s)
2D-DSA	3D-DSA					
0.15	0.46	68.4	1.12 ± 0.12	0.17 ± 0.02	3	23.1
0.31	0.46	95.4	1.10 ± 0.12	0.17 ± 0.003	12	8.0
0.62	0.46	96.4	1.13 ± 0.15	0.17 ± 0.004	16	3.7
1.23	0.46	74.9	1.13 ± 0.14	0.17 ± 0.004	0	4.4

Registration with Same Resolution. Based on the previous results, we resampled the 2D projection images to the original resolution of the 3D volume data and repeated previous registration experiments. Both, the results for the initial translation (Fig. 2(b)) and the results for the given initial displacements (Table 2) confirm our assumption. For the latter, a success rate of 98.3% and 99.5% was achieved with the LAT and AP images, respectively, and a capture range of 20 mm. In addition, a mean value and a standard deviation of the mRPD of 0.17 mm ± 0.004 mm for the LAT images and 0.12 mm ± 0.003 mm for the AP images as well as an mTRE of 1.06 mm ± 0.15 mm and 0.55 mm ± 0.14 mm for the LAT and AP images were achieved. Since we use a publicly accessible database, we can directly compare the results with other results found in the literature for this database. The results achieved with our proposed method are comparable to the results from [12] and much better than the reported results in [7,11]. Except for the mean value and standard deviation of the mTRE for the LAT images, our results are the best results for all compared methods. The runtime for a single registration is not directly comparable as it is not always reported and even if, different hardware is used. The extensive DRR generation is done on a graphics card, but other than that no further runtime optimization was done. Still, registration is fast on of-the-shelf hardware.

Experiment Finest Resolution. As Table 1 already indicates, the registration on fine level is time consuming. This rises the question how the accuracy behaves if fine levels are omitted. We have also looked into this. Table 3 shows the results

Table 2. Results for the registration of a 3D-DSA to a 2D-DSA from LAT or AP view averaged over all 10 datasets of the proposed *DRR-NGF-ML* method compared to the results of other state-of-the-art methods reported in [7,11,12]. Given are the Success Rate (SR), the mean and standard deviation of the mTRE and mRPD, the capture range (CR) and the mean amount of time for one registration. Missing values are marked with a " - ".

View	Method	SR (%)	mTRE (mm)	mRPD (mm)	CR (mm)	Time (s)
LAT	MGP+BGB [7]	79.5	-	0.28 ± 0.21	6	15.3
	PB-BGC [11]	82.2	-	0.51 ± 0.29	9	**1.8**
	PPC-LADR [12]	95.6	0.91 ± 0.50	0.22 ± 0.08	16	-
	PPC-MCCR [12]	98.3	**0.64 ± 0.31**	0.23 ± 0.08	18	-
	DRR-NGF-ML	***99.3***	*1.06 ± 0.15*	***0.17 ± 0.004***	*20*	*4.7*
AP	MGP+BGB [7]	95.5	-	0.28 ± 0.19	12	11.5
	PPC-LADR [12]	97.3	0.57 ± 0.38	0.15 ± 0.08	16	-
	PPC-MCCR [12]	99.4	0.59 ± 0.27	0.16 ± 0.08	**20**	-
	DRR-NGF-ML	***99.5***	***0.55 ± 0.14***	***0.12 ± 0.003***	*20*	*3.6*

Table 3. Results for the registration of a 3D-DSA to a 2D-DSA from LAT view averaged over all 10 datasets with different resolutions of the finest level of both volume and projection.

Resolution finest level (mm)	SR (%)	mTRE (mm)	mRPD (mm)	CR (mm)	Time (s)
0.46	99.3	1.06 ± 0.15	0.17 ± 0.004	20	4.7
0.93	99.2	0.96 ± 0.20	0.17 ± 0.005	20	3.2
1.9	95.1	0.74 ± 0.29	0.18 ± 0.006	14	2.6

for the case of adjusted resolutions and for omitting the first and second finest levels. The success rate, accuracy and capture range are almost identical if the finest level is omitted, only the average registration time decreases significantly. If the two finest levels are omitted, the runtime further decreases, but also success rate and the detection range decreases significantly, too. Thus omitting the finest level seems to achieve the best trade-off between accuracy and speed.

4   Discussion

In this paper we discussed the relation between projection resolution and volume resolution. The main conclusion is that the resolutions should be comparable. One observation that may be surprising is that the use of finer resolutions does not bring any advantage, and may even bring disadvantages if the resolutions are not comparable. Another observation is that for reasons of acceleration, the finest level can be omitted and the accuracy for this particular database is not lost. Besides the investigations about the multilevel strategies, we proposed an

efficient multilevel 2D-3D registration method using the NGF distance measure yielding results that are comparable and even superior to the state-of-the-art.

References

1. Goudeketting, S.R., Heinen, S.G., Ünlü, Ç., et al.: Pros and cons of 3D image fusion in endovascular aortic repair: a systematic review and meta-analysis. J. Endovasc. Therapy **24**(4), 595–603 (2017). https://doi.org/10.1177/1526602817708196

2. Haber, E., Modersitzki, J.: Intensity gradient based registration and fusion of multi-modal images. In: Larsen, R., Nielsen, M., Sporring, J. (eds.) MICCAI 2006. LNCS, vol. 4191, pp. 726–733. Springer, Heidelberg (2006). https://doi.org/10.1007/11866763_89

3. Jonic, S., Thévenaz, P., Unser, M.A.: Multiresolution-based registration of a volume to a set of its projections. In: Medical Imaging 2003: Image Processing, vol. 5032, pp. 1049–1052. International Society for Optics and Photonics (2003). https://doi.org/10.1117/12.480241

4. Van de Kraats, E.B., Penney, G.P., Tomazevic, D., Van Walsum, T., Niessen, W.J.: Standardized evaluation methodology for 2-D-3-D registration. IEEE Trans. Med. Imaging **24**(9), 1177–1189 (2005). https://doi.org/10.1109/TMI.2005.853240

5. Maes, F., Vandermeulen, D., Suetens, P.: Comparative evaluation of multiresolution optimization strategies for multimodality image registration by maximization of mutual information. Med. Image Anal. **3**(4), 373–386 (1999). https://doi.org/10.1016/s1361-8415(99)80030-9

6. Markelj, P., Tomaževič, D., Likar, B., Pernuš, F.: A review of 3D/2D registration methods for image-guided interventions. Med. Image Anal. **16**(3), 642–61 (2012). https://doi.org/10.1016/j.media.2010.03.005

7. Mitrović, U., Špiclin, Ž., Likar, B., Pernuš, F.: 3D–2D registration of cerebral angiograms: a method and evaluation on clinical images. IEEE Trans. Med. Imaging **32**(8), 1550 (2013). https://doi.org/10.1109/TMI.2013.2259844

8. Mitrović, U., Likar, B., Pernuš, F., Špiclin, Ž.: 3D–2D registration in endovascular image-guided surgery: evaluation of state-of-the-art methods on cerebral angiograms. Int. J. Comput. Assist. Radiol. Surg. **13**(2), 193–202 (2017). https://doi.org/10.1007/s11548-017-1678-2

9. Munbodh, R., et al.: Automated 2D–3D registration of a radiograph and a cone beam CT using line-segment enhancement. Med. Phys. **33**(5), 1398–1411 (2006). https://doi.org/10.1118/1.2192621

10. Rühaak, J., Heldmann, S., Kipshagen, T., Fischer, B.: Highly accurate fast lung CT registration. In: SPIE Medical Imaging 2013: Image Processing, February 2013. https://doi.org/10.1117/12.2006035

11. Špiclin, Ž., Likar, B., Pernuš, F.: Fast and robust 3D to 2D image registration by backprojection of gradient covariances. In: Ourselin, S., Modat, M. (eds.) WBIR 2014. LNCS, vol. 8545, pp. 124–133. Springer, Cham (2014). https://doi.org/10.1007/978-3-319-08554-8_13

12. Wang, J., et al.: Dynamic 2-D/3-D rigid registration framework using point-to-plane correspondence model. IEEE Trans. Med. imaging **36**(9), 1939–1954 (2017). https://doi.org/10.1109/TMI.2017.2702100